Current improvements in interpretation of posterior capsular opacification images

Andrew P. Papliński
Computer Science and Software Engineering,
Monash University, Victoria 3800, Melbourne, Australia
app@csse.monash.edu.au

Abstract

We present application of curvature-driven min/max flow and anisotropic diffusion in processing posterior capsular (PCO) images. PCO images present the back surface of the lens implanted during cataract surgery and are used to monitor the state of patient vision. Our standard segmentation technique which based on variance based co-occurrence matrices often requires an enhancement of variance images prior to segmentation. A number of enhancement methods are based on partial differential equations, and we present two such methods. We demonstrate that the curvature-driven flow seems to enhance better the significant edges in the image, whereas the anisotropic diffusion seems to work better with smoothing intra-regional image features.

1 Introduction

In this paper we present our recent work on interpretation of the Posterior Capsular Opacification (PCO) images.

The PCO images present the back surface of the lens implanted during cataract operation and are used to monitor the post-cataractal state of patient's vision, which may be affected by the growth of epithelial cells inside the posterior capsule [1, 2, 3]. Interpretation of the PCO images is based on their segmentation into areas of low and high texture. The low-texture areas represent the transparent part of the eye posterior capsule behind the implanted lens, whereas the high-texture areas are equivalent to the opaque part of the capsule. Our standard method of segmentation of the PCO images presented in papers[4, 5, 6, 7, 3] is based on the application of a directional variance operator and co-occurrence arrays. The method works very efficiently in the majority of cases, but there are a non-negligible number of cases where the segmentation error is unacceptably high.

In this work we compare two non-linear methods of image enhancement based on application of partial differential equations, namely, the curvature-driven min/max flow [8, 9] and an anisotropy diffusion method [10]. Comprehensive bibliography on variational methods can be found in [11] and [9]. By image enhancement we understand processing of an image in such a way to maintain or possibly enhance sharp edges of an image and to remove small intra-regional features considered to be noise, that is, to smooth intensity inside image regions. This work is related to our previous work presented in [12, 13, 14] on application of partial differential equations in interpretation of the PCO images.

2 Curvature-Driven Min/Max Flow

The curvature-driven evolution of an image $u(\mathbf{x},t)$ is described by the following partial differential equation [9]:

$$\frac{\partial u(\mathbf{x},t)}{\partial t} = F(\kappa(\mathbf{x},t))|\nabla u(\mathbf{x},t)| \ , \quad \kappa = \text{div}(\frac{\nabla u}{|\nabla u|}) \tag{1}$$

where $u(\mathbf{x},t)$ is an evolving image intensity, ∇u is its gradient, and $F(\kappa)$ is an appropriately selected "speed" function of the image curvature, κ.

Early examples of the speed functions are considered, among others, in [15] where $F=\kappa$, and in [16] where $F=\kappa^{1/3}$. In each of this schemes, all image information would be eventually filtered out if iterations are performed continuously. This is the result of the Grayson's theorem [17, 18] which says that each contour shrinks to zero and disappears.

An elegant way to address this problem is a min/max flow method introduced in [8, 9]. Under the min/max principle the speed function, $F(\kappa)$, is of the following form

$$F(\kappa(\mathbf{x})) = \begin{cases} \max(\kappa,0) & \text{if } \text{ave}_\rho(u(\mathbf{x})) < \text{ave}_\perp(u(\mathbf{x})) \\ \min(\kappa,0) & \text{otherwise} \end{cases} \tag{2}$$

where $\text{ave}_\rho(u(\mathbf{x}))$ is an average intensity in the neighborhood of a pixel $\mathbf{x}$ of a radius ρ, and $\text{ave}_\perp(u(\mathbf{x}))$ is an average intensity on the direction perpendicular to the gradient, that is, tangent to the iso-intensity contour line. It can be observed [8, 9] that flow under $F=\max(\kappa,0)$ (positive-only curvature) smoothes away all image details, whereas, flow driven by $F=\min(\kappa,0)$ (negative-only curvature) preserves the strong edges of the image.

The average intensity in the neighborhood of a pixel $\mathbf{x}$ of a radius ρ, $\text{ave}_\perp(u(\mathbf{x}))$, is calculated as a convolution

of the evolving image, $u(\mathbf{x})$, with a $\rho \times \rho$ Gaussian mask of the variance $\sigma^2 = 0.5\rho^2$. Increasing the radius, ρ, the amount of smoothing is in general increased.

In order to calculate the average intensity along the line tangent to the iso-intensity contour we first note that such a tangent line can, in general, go in between the image pixels. Therefore, in the average we include intensities at the pixels located at a strip of a given width around the tangent line. The intensities are weighted with the distance from the tangent line, which can be calculated as the projection of the location vector, $\mathbf{x}$, on the gradient, ∇u. The average is taken only on the segment of the tangent line inside the disk of the radius ρ.

The min/max flow as described by eqns (1), (2) is applied to a PCO image. The original image and an image after 40 iterations are shown in Figure 1.
From Figure 1 b it can be noticed that the borders between areas of unified intensity have been enhanced, and the noise from inside the image regions has been filtered out. The enhancement of the region borders occurs through their thinning and averaging their curvatures. The degree of smoothing is controlled by the radius of the averaging disk, ρ.

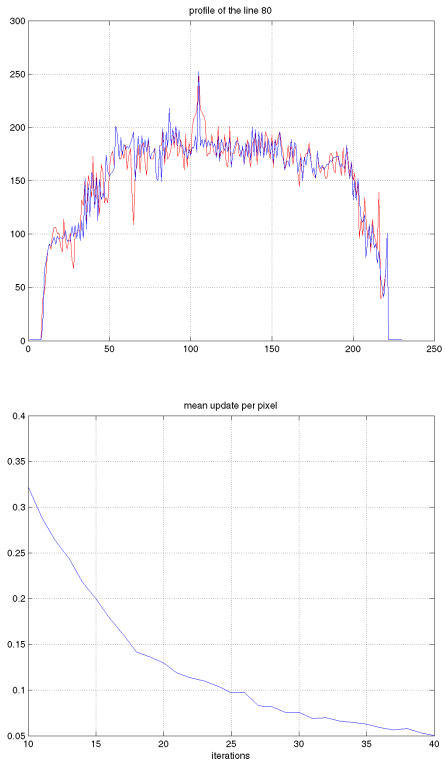

Figure 2: top: The profile of the line 80. botom: The mean update per pixel during iterations

Some additional features of the max/min curvature flow can be observed from Figure 2 where a cross-section of the image intensity along the specified line has been shown. Note that the large gradient has been increased by increasing the slope of the line. This is equivalent to the thinning an image region. Small variations of the gradient have been non-linearly averaged. It is also important to note from the right plot in Figure 2 that the mean update per pixel is being exponentially reduced which demonstrates the convergence of the algorithm.

3 Anisotropic diffusion method

An anisotropic diffusion equation is similar to the previously considered curvature-based equation in that that it is also comprised of only first and second spatial derivatives, and that it is also a nonlinear partial differential equation. A standard form of an anisotropic diffusion equation is as follow:

$$\frac{\partial u(\mathbf{x},t)}{\partial t} = \text{div}(L(\mathbf{x},t)\nabla u(\mathbf{x},t)) \qquad (3)$$

where $L(\mathbf{x},t)$ is a 2×2 diffusion matrix controlling anisotropy. In a special case when the anisotropy matrix is identity, eqn (3) describes isotropic diffusion which in terms of the image processing smoothes all image features away. The anisotropic diffusion equation describes image changes which are proportional to the sum of spatial derivatives of the diffusion vector, $v = L \cdot \nabla u$. In particular, when the diffusion vector becomes zero, the image intensity reaches its steady state and the image pixel remains unchanged. Note that the diffusion vector, v, becomes zero when either the gradient is zero, or the diffusion matrix is the orthogonal projection of the gradient.

Following [10] we exploit two basic ideas which are important from the point of view of obtaining image enhancement behaviour of the algorithm based on eqn (3). The first idea is that the anisotropy vector should steadily reach the value of zero, and the second one is that such a state should be obtained either by the diffusion matrix being the orthogonal projection of the image gradient which gives $v = L \cdot \nabla u = 0$, or by the image gradient approaching zero. This can be achieved by means of the following relaxation equation for the anisotropy matrix:

$$\frac{\partial L(\mathbf{x},t)}{\partial t} + \frac{1}{\tau}L(\mathbf{x},t) = \frac{1}{\tau}F(\nabla u(\mathbf{x},t)) \qquad (4)$$

where $F(\nabla u(\mathbf{x},t))$ is a 2×2 anisotropy "force" matrix, and τ is a time constant which determines the speed of relaxation of the diffusion matrix. Eqn (4) describes evolution of the diffusion matrix from its initial value, say $L = I$ to the one which is enforced by the F matrix. The specific form of the force matrix, F, will be selected based on the value of of the magnitude of the image gradient. If the image gradient exceeds a threshold parameter, s, then the matrix F will be the orthogonal projection of the gradient, otherwise its form will

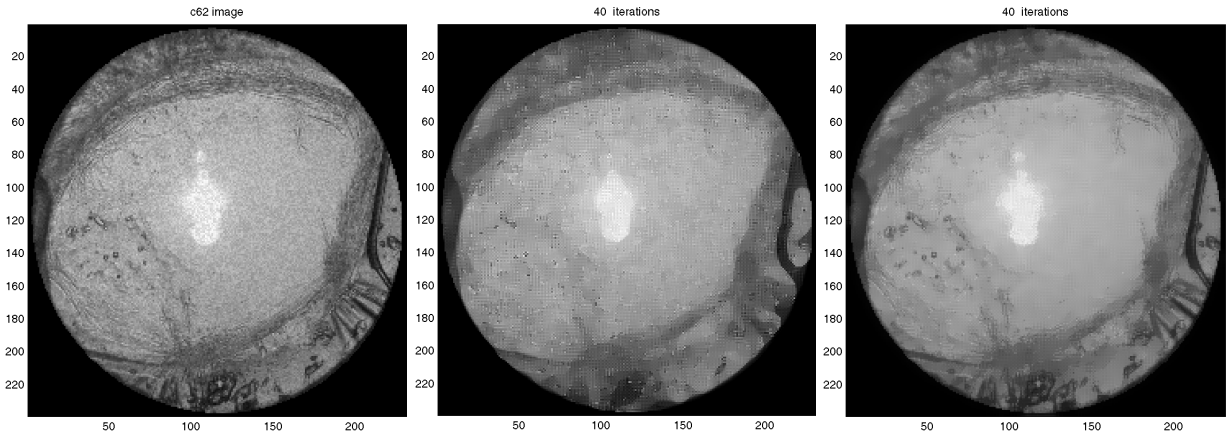

Figure 1: The original noisy image (a), the image after 40 iterations using the min/max flow (b) and the anisotropic diffusion (c).

ensure isotropic diffusion, which smoothes the image in the areas where the gradient falls below the threshold parameter. Details are presented in [19]

The set of equations (3), (4) gives a stable solution to the anisotropic diffusion equation which ensures maintaining strong edges in the image and flattening image features which are considered to be irrelevant. For a rigorous mathematical treatment the reader is referred to [10].

The results of processing the test image are presented in Figure 1 c. From Figure 1 c it can be observed that the borders between image regions considered to be significant with respect to the stiffness threshold, s, have been maintained, whereas, the intra-regional features have been strongly filtered out. This results in a segmentation-like processing of an image. Some additional aspects of the anisotropic diffusion iterations have been presented in Figure 3.

From Figure 3 it can be noticed that for the selected parameters β and τ low-pass filtering is very prominent. The convergence of the algorithm characterised by the mean update per pixel is similar to that of the curvature driven min/max flow.

Comparing the curvature driven min/max flow and the anisotropic diffusion we can note that the first method actively enhances the inter-regional borders by modifying the curvature of the border curves. The second method appears to be better in filtering out the intra-regional features. Both algorithms maintain the average values of the image intensity, which is a very convenient feature, and converge to a steady-state.

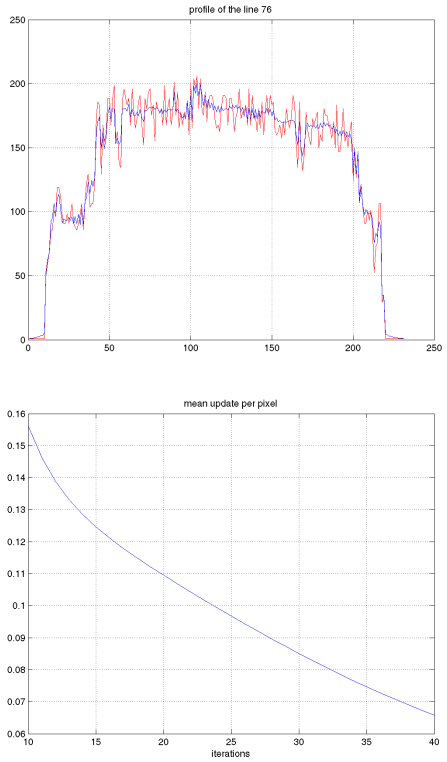

Figure 3: top: The profile of the line 80. bottom: The mean update per pixel during iterations

Concluding remarks

Two variational methods, namely, a curvature-driven min/max flow and anisotropic diffusion can be used to enhance posterior capsular opacification images. In the qualitative sense it seems that the curvature-driven method seems to enhance better the significant edges in the image, whereas the anisotropic diffusion seems to work better with smoothing intra-regional image features.

Acknowledgments

The authors would like to express their gratitude to Mr D. J. Spalton, Clinical Director of the Department of Ophthalmology of St Thomas' Hospital London, for the

specification of the problem, the provision of the image data and many useful discussions.

References

[1] M. V. Pande, P. G. Ursell, D. J. Spalton, and S. Kundaiker, "High resolution digital retroillumination imaging of the posterior lens capsule after cataract surgery," *J. Cataract Refract. Surg.*, vol. 23, pp. 1521–1527, 1997.

[2] D. S. Friedman, D. D. Duncan, M. Beatriz, and S. K. West, "Digital image capture and automated analysis of posterior capsular opacification," *Invest. Ophthalmology Vis. Sci.*, vol. 40, pp. 1715–1726, July 1999.

[3] S. A. Barman, J. F. Boyce, and A. P. Papliński, "Automatic quantification of posterior capsular opacification," in *Proceedings of SPIE: Medical Imaging 2000*, vol. 3979, (San Diego, California, USA), pp. 119–128, February 2000.

[4] A. P. Papliński and J. F. Boyce, "Segmentation of a class of ophthalmological images using a directional variance operator and co-occurrence arrays," *Optical Engineering*, vol. 36, pp. 3140–3147, November 1997.

[5] A. P. Papliński, "Directional filtering in edge detection," *IEEE Trans. Image Proc.*, vol. 7, pp. 611–615, April 1998.

[6] A. P. Papliński and J. F. Boyce, "Co-occurrence arrays and edge density in segmentation of a class of ophthalmological images," in *Proceedings of the 4rd Conference on Digital Image Computing: Techniques and Applications, DICTA97*, (Auckland,), pp. 521–528, December 1997.

[7] A. P. Papliński and J. F. Boyce, "Tri-directional filtering in processing a class of ophthalmological images," in *Proceedings of the IEEE Region 10 Annual Conference, TENCON'97*, (Brisbane), pp. 687–690, December 1997.

[8] R. Malladi and J. A. Sethian, "Image processing: Flows under min/max curvature and mean curvature," *Graphical Models and Image Processing*, vol. 58, no. 2, pp. 127–141, 1996.

[9] J. A. Sethian, *Level Set Methods and Fast Marching Methods*. Cambridge University Press, 2nd ed., 1999.

[10] G. H. Cottet and M. El Ayyadi, "A Voltera type model for image processing," *IEEE Transactions on Image Processing*, vol. 7, pp. 292–303, March 1998.

[11] V. Caselles, J.-M. Morel, G. Sapiro, and A. Tannenbaum, "Introduction to the special issue on partial differential equations and geometry driven diffusion in image processing," *IEEE Transactions on Image Processing*, vol. 7, pp. 269–273, March 1998.

[12] A. P. Papliński, "Curvature-driven min/max flow and anisotropic diffusion in image enhancement," in *Proceedings of the 2nd International Symposium on Advanced Concepts for Intelligent Vision Systems (ACIVS'2000)*, (Baden-Baden, Germany), pp. 41–48, The International Institute for Advanced Studies in Systems Research and Cybernetics, August 2000.

[13] A. P. Papliński and J. F. Boyce, "Processing a class of ophthalmological images using an anisotropic diffusion equation," in *Proceedings of the 2nd Annual IASTED International Conference on Computer Graphics and Imaging (CGIM'99)*, (Palm Springs, California, USA), pp. 134–138, October 1999.

[14] A. P. Papliński and J. F. Boyce, "Application of an anisotropic diffusion equation in processing a class of ophthalmological images," in *Proceedings of the International Symposium on Advanced Concepts for Intelligent Vision Systems (ACIVS'99)*, (Baden-Baden, Germany), pp. 33–39, The International Institute for Advanced Studies in Systems Research and Cybernetics, August 1999.

[15] L. Alvarez and L. Mazorra, "Image selective smoothing and edge detection by non-liner diffusion," *SIAM J. Num. Anal.*, vol. 29, no. 3, pp. 845–866, 1992.

[16] G. Sapiro and A. Tannenbaum, "Image smoothing based on affine invariant flow," in *Proceedings of the Conference on Information Sciences and Systems*, (Johns Hopkins University), March 1993.

[17] M. Grayson, "The heat equation shrinks embedded plane curves to round points," *J. Diff. Geom.*, no. 26, p. 285, 1987.

[18] M. Grayson, "A short note on the evolution of surfaces via mean curvatures," *J. Diff. Geom.*, p. 555, 1989.

[19] A. P. Papliński, J. F. Boyce, and S. A. Barman, "Improvements in interpretation of posterior capsular opacification (PCO) images," in *Proceedings of SPIE: Medical Imaging 2000*, vol. 3979, (San Diego, California, USA), pp. 951–958, February 2000.